Biochemical Systematics and Ecology 40 (2012) 75–85

Contents lists available at SciVerse ScienceDirect

Biochemical Systematics and Ecology

journal homepage: www.elsevier.com/locate/biochemsyseco

Molecular and catalytic characterization of a phi class glutathione transferase from *Cathaya argyrophylla*

Tao Wei [a,b], Cai-Ling Wang [c], Hong-Na Kao [a,b], Hai-Ling Yang [c], Xiao-Ru Wang [a,d], Qing-Yin Zeng [a,*]

[a] State Key Laboratory of Systematic and Evolutionary Botany, Institute of Botany, Chinese Academy of Sciences, 100093 Beijing, China
[b] Graduate University of the Chinese Academy of Sciences, Beijing 100049, China
[c] College of Life Sciences and Biotechnology, Beijing Forestry University, 100083 Beijing, China
[d] Department of Ecology and Environmental Science, Umeå University, SE-901 87 Umeå, Sweden

ARTICLE INFO

Article history:
Received 17 August 2011
Accepted 8 October 2011
Available online 4 November 2011

Keywords:
Cathaya argyrophylla
Gymnosperm
Enzyme characterization
Site-directed mutagenesis
Protein structure

ABSTRACT

Plant phi class glutathione transferases (GSTs) play important roles in stress tolerance and detoxification metabolism. This study reports the cloning, expression and biochemical characteristics of a phi GST gene (*Ca*GSTF) from the endemic and endangered conifer *Cathaya argyrophylla*. The recombinant *Ca*GSTF showed GSH-conjugating activity towards the substrate NBD-Cl and CDNB. Kinetic analysis revealed low catalytic efficiency with a k_{cat}/K_m^{GSH} value of 9.82 $mM^{-1}S^{-1}$. The *Ca*GSTF proved to be a thermolabile enzyme, at 40 °C the enzyme's activity was nearly abolished. Site-directed mutagenesis revealed that Ser12, Lys42, Ile55, Glu67 and Ser68 of *Ca*GSTF are critical components of glutathione-binding sites that contribute to the enzyme's catalytic activity. Compared to other plant phi GSTs and conifer tau GSTs, *Ca*GSTF showed a narrow substrate spectrum, low catalytic efficiency and thermolability. These atypical properties suggest the enzyme may have a limited functional role in the organism's adaptation to environmental stresses in the subtropical regions.

1. Introduction

Glutathione transferases (GSTs, EC2.5.1.18) are involved in the phase II detoxification metabolism. These intracellular proteins are found in most aerobic eukaryotes and prokaryotes, and protect cells against chemical-induced toxicity and stress by catalyzing the S-conjugation between the thiol group of glutathione and an electrophilic moiety in the hydrophobic and toxic substrate (Dirr et al., 1994). In plant, GSTs are mainly grouped into seven classes, phi, zeta, tau, theta, lambda, DHAR (dehydroascorbate reductases) and TCHQD (tetrachlorohydroquinone dehalogenase) (Frova, 2003; Öztetik, 2008). Recently, based on structural similarities, the γ-subunit of the eukaryotic translation elongation factor 1B (EF1Bγ) is also being regarded as a member of the GST family (Oakley, 2005). The zeta and theta GSTs are found both in plants and animals, but the phi, tau, lambda and DHAR GSTs are considered as unique to plants. GST isoenzymes belonging to the same class show >40% identity in their primary structure, whereas enzymes belonging to the different classes generally have less than 25% sequence identity (Frova, 2003). The phi GSTs, which are abundant in plant, can conjugate a diverse array of xenobiotics, such as various toxic compounds, herbicides and herbicide safener (Basantani and Srivastava, 2007; Cummins et al., 2003; Dixon et al., 1997; Wu et al., 1999). These GSTs participate in endogenous cellular metabolism by functioning as glutathione peroxidases that

* Corresponding author. Tel.: +86 10 62836440; fax: +86 10 62590843.
E-mail address: qingyin.zeng@ibcas.ac.cn (Q.-Y. Zeng).

0305-1978/$ – see front matter © 2011 Elsevier Ltd. All rights reserved.
doi:10.1016/j.bse.2011.10.010

counteract oxidative stress (Cummins et al., 2003; McGonigle et al., 2000). Plant phi GSTs are also involved in cell signalling during stress responses (Edwards et al., 2000; Sappl et al., 2004). Up to date, there is virtually no information on the molecular characteristics of phi class GSTs in gymnosperms. Gymnosperms represent a large group of plants with a long evolutionary history. Most of the gymnosperms such as conifers are important forest-forming species. Over their lifespans the conifers have to cope with severe stresses including temperature fluctuations, drought, elevated ozone level, halogenated hydrocarbons and other air pollutants. The presence of enzymes that can detoxify these compounds and respond to natural stresses is clearly beneficial for the adaptation of conifer trees. Currently, the only available molecular and biochemical data on GSTs in conifers are from four tau GSTs and one zeta GST cloned from pines (Oztetik, 2005; Zeng et al., 2005; Zeng and Wang, 2006), and three unclassified GSTs purified directly from needles of pine and spruce (Schroder and Berkau, 1993; Schroder et al., 1990; Schroder and Rennenberg, 1992).

Cathaya argyrophylla Chun et Kuang is an extremely endangered conifer with an estimate of less than 2000 trees remaining in restricted and isolated regions of subtropical mountains in China (Wang and Ge, 2006). *C. argyrophylla* has a unique taxonomic position in Pinaceae; it forms the only monospecific genus in the family (Wu and Peter, 1999). Conservation biologists are interested in the evolutionary processes that have led to the endemic situation. Studies on phi class GSTs in *C. argyrophylla* could provide an additional line of information useful for assessing the mechanisms of the species' decline. In addition, due to the scarce data on GST gene family in gymnosperms, more studies on this group of plants would advance our understanding on the patterns of divergence in structure and function of the gene family between angiosperms and gymnosperms. In this study, we report for the first time the cloning of a phi class GST from *C. argyrophylla*. Through enzyme assays, phylogenetic analysis and structural modelling, we provide a detailed characterization of the gene and the enzyme in *C. argyrophylla*.

2. Materials and methods

2.1. Molecular cloning

The GenBank EST database was searched using the BLAST program (http://blast.ncbi.nlm.nih.gov/Blast.cgi) with the rice phi GST protein *Os*GSTF2 (GenBank accession no. AAC64007) as query sequence. Two *Picea glauca* EST sequences (GenBank accession nos. EX310023 and DV983884) encoding an unknown protein with high similarity to the query GST sequence were identified. Based on the two EST sequences, two primers (PgGSTF-CL1: 5′-GCTGTTTGAGAGAGCCTGATA-3′ and PgGSTF-CL12: 5′-GCACGACTTCCATTTATTTG-3′) were designed to amplify a phi GST cDNA in *C. argyrophylla*.

Fresh needles of *C. argyrophylla* were used for total RNA isolation using a TIANGEN PLANT RNA Kit (Tiangen Biotech, Beijing, China). The first strand cDNA was synthesized using a TaKaRa RNA PCR Kit (AMV) Ver.3.0 (Takara, Shiga, Japan). PCR was performed in a volume of 50 μl containing 2 μl of the first strand cDNA, 10 μl of TaKaRa 5 × PCR buffer, 0.25 μl TaKaRa ExTaq and 10 pmol of each primer (PgGSTF-CL1/2). PCR conditions were optimized to consist of an initial denaturation of 3 min at 94 °C, followed by 35 cycles of 30 s at 94 °C, 40 s at 50 °C and 60 s at 72 °C, followed by a final extension of 5 min at 72 °C. A PCR product (about 850 bp) recovered from 1% agarose gel was cloned into the pGEM-T Vector (Promega, Madison, WI, USA) and sequenced in both directions. This cDNA from *C. argyrophylla* was named *Ca*GSTF.

To obtain the genomic sequence of the *Ca*GSTF gene, genomic DNA of *C. argyrophylla* was isolated from needles using a TIANGEN DNeasy Plant Mini Kit (Tiangen Biotech, Beijing, China). The genomic sequence of the *Ca*GSTF was amplified using the primers PgGSTF-CL1/2. The amplification conditions were as described above. PCR product was cloned and sequenced in both directions. The genomic sequence of *Ca*GSTF has been deposited in GenBank with accession no. FJ517560.

2.2. Phylogenetic analysis

The protein sequence of *Ca*GSTF was deduced from the cDNA, aligned with other plant GSTs using ClustalX software (Thompson et al., 1997) and further adjusted manually using BioEdit (Hall, 1999). Sequence divergence and phylogenetic analysis were performed using MEGA v.4.0 (Tamura et al., 2007). The neighbour-joining (NJ) method of phylogenetic tree reconstruction was used to establish the genetic relationships between *Ca*GSTF and other major classes of plant GSTs, with 1000 bootstrap replicates and distant animal GSTs as outgroup using MEGA v.4.0.

2.3. Expression and purification of recombinant CaGSTF

The open reading frame (including the stop codon) of the cDNA encoding *Ca*GSTF was amplified by PCR with the upstream primer 5′-TGGATCCATGGCAACGATCACGTTAT-3′ and the downstream primer 5′-TAAGCTTTTATCATTTTGGTCCTTTCTCA-3′ (*Bam*HI and *Hind*III sites underlined, respectively). The PCR product was digested with *Bam*HI and *Hind*III and subcloned into the plasmid expression vector pET30a (Novagen, Madison, WI, USA), which provide the correct reading frame and a 6 × His-tag at the N-terminus. The resultant plasmids were used to transform *Escherichia coli* BL21-Tuner. Colonies containing the appropriate insert were identified by sequencing. Site-directed mutagenesis of *Ca*GSTF was performed as described by Zeng and Wang (2005).

An overnight culture of *E. coli* BL21 containing the recombinant pET30a plasmid was diluted 1:100 and grown until the optical density (A_{600}) reached 0.5. IPTG was added to the culture at a final concentration of 0.1 mM and incubation was continued for a further overnight at 20 °C. Bacteria were harvested by centrifugation at 5000 g for 3 min at 4 °C, resuspended

in binding buffer (20 mM sodium phosphate, 0.5 M NaCl, 20 mM imidazole, pH 7.5), and disrupted by cold sonication. The particulate material was removed by centrifugation at 10,000 g for 10 min at 4 °C, and the supernatant was loaded onto a Ni Sepharose High Performance column (Amersham Pharmacia Biotech) that had been pre-equilibrated with binding buffer. The over-expressed protein that bound to the Ni Sepharose High Performance column was eluted with elution buffer (20 mM sodium phosphate, 0.5 M NaCl, 0.5 M imidazole, pH 7.5). The purified recombinant protein was desalted using a PD-10 column (Amersham Pharmacia Biotech) in 10 mM Tris–HCl buffer, pH 7.0.

2.4. Enzyme assays and kinetic studies

The GST activities towards 1-chloro-2,4-dinitrobenzene (CDNB), 1,2-dichloro-4-nitrobenzene (DCNB) and 4-nitrobenzyl chloride (NBC) were measured as described by Habig et al. (1974), and activity towards 7-chloro-4-nitrobenzo-2-oxa-1,3-diazole (NBD-Cl) as described by Ricci et al. (1994), and activity towards hydroxyethyl disulphide (HED), dehydroascorbate (DHA) and cumene hydroperoxide (Cum-OOH) were measured as described by Edwards and Dixon (2005). All assays were carried out at 25 °C. SDS–PAGE was performed on 10% separating gels and 5% stacking gel. The dependence of GST activity on pH was measured as reported by Yuen and Ho (2001). Thermal stability of *Ca*GSTF was measured by incubating the enzyme for 15 min at various temperatures from 25 °C to 50 °C at 5 °C intervals. GST activity towards NBD-Cl was determined at the end of each incubation. Protein concentrations were determined by measuring the absorbance at 280 nm (Layne, 1957).

The fluorescence dye 8-anilino-1-naphthalene-sulfonate (ANS) is a valuable probe for the detection and analysis of structural changes in proteins (Schonbrunn et al., 2000). In order to detect structural changes between the mutant and wild-type enzymes, The ANS binding assay was monitored using a HITACHI F-4500 FL Spectrophotometer. 100 μl of 2 mM ANS was added to a final concentration of 0.05 mg/ml enzyme (1 M sodium phosphate buffer, pH 6.5) in a 1 ml reaction mixture. A total of three scans each for blank and sample were recorded and averaged for each enzyme. Reported spectra are the means from at least three independent experiments.

The enzyme's steady state kinetics were studied in assays with various concentrations of GSH and NBD-Cl. The apparent K_m value for GSH was determined using a GSH range from 0.1 to 1.0 mM at fixed NBD-Cl concentration of 1.0 mM. The apparent K_m value for NBD-Cl was determined using a NBD-Cl range from 0.1 to 1.0 mM at fixed GSH concentration of 1.0 mM. The kinetic parameters were derived using non-linear regression as implemented in the Hyper32 program available from http://www.liv.ac.uk/~jse/software.html

2.5. Homology modelling

X-ray structure of the maize phi GST protein (Protein Data Bank code No.: 1axd) was used as template for constructing a structure model of *Ca*GSTF. Sequences were aligned using Align 2D structure alignment program (Homology Module, InsightII). Structures were built using the Modeler module of InsightII. All structures were verified by profile-3D program of InsightII. The structure models were selected according to model evaluation score calculated by Profile-3D. The three-dimensional structural image was generated using the program Swiss-Pdb Viewer.

3. Results

3.1. Sequence characterization of the CaGSTF gene

The mRNA from needles of *C. argyrophylla* was isolated and reverse transcribed into cDNA. A 839 bp DNA fragment was amplified. The full nucleotide and deduced amino acid sequence of this cDNA are shown in Fig. 1. This cDNA sequence was named *Ca*GSTF (GenBank accession no.: FJ517561). It contains a 654 bp open reading frame (excluding the stop codon), 7 bp of 5′ non-coding sequence and 175 bp of 3′ non-coding sequence. This cDNA encodes a peptide of 218 residues that has a predicted molecular mass of 24.29 kDa. The deduced protein sequence showed a low sequence identity (<22%) to tau and zeta GSTs cloned from pines (Oztetik, 2005; Zeng et al., 2005; Zeng and Wang, 2006). The genomic sequence of *Ca*GSTF spans 1048 bp (GenBank accession no.: FJ517560) and contains two introns of 98 bp and 111 bp, respectively (Fig. 1). This two-intron structure has been observed in rice and *Arabidopsis* phi class GSTs (Dixon et al., 2002; Soranzo et al., 2004).

The *Ca*GSTF protein sequence was used in a homology analysis using the BLAST program (http://www.ncbi.nlm.nih.gov/blast/Blast.cgi), and it showed a high similarity to the plant phi class GSTs. A multiple alignment of the *Ca*GSTF with other eight phi GSTs is shown in Fig. 2. *Ca*GSTF has 40–54% sequence identity to other plant phi GSTs listed in Fig. 2. Phylogenetic analysis of the plant GSTs protein sequences revealed a distinct subdivision of the six GSTs classes (Fig. 3). *Ca*GSTF was placed within the phi class with strong bootstrap support (100%). The GSTs of the theta, zeta, tau, lambda and DHAR classes were also grouped with strong bootstrap support (100%). Thus, based on the amino acid sequence similarity and phylogenetic division, the *Ca*GSTF should be classified as a phi class GST.

3.2. Identification of the GSH-binding sites of the CaGSTF

The three-dimensional structure of *Ca*GSTF (Fig. 4A) was modelled based on the X-ray structure of the maize phi GST protein (Protein Data Bank code No.: 1axd). The structure was further examined by program Profile-3D. Except for residues

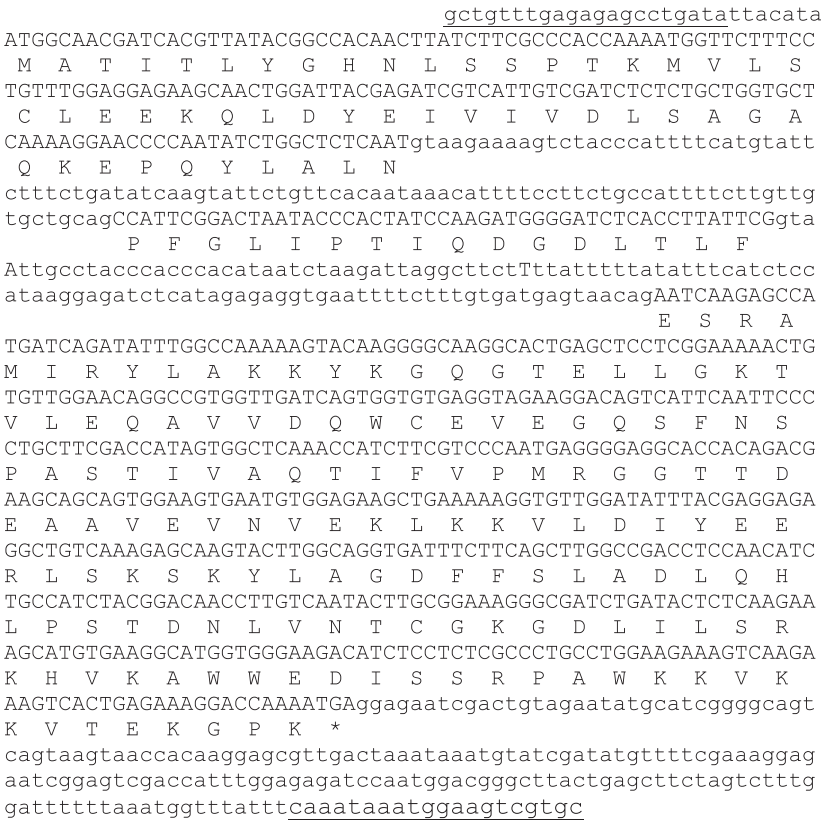

Fig. 1. Nucleotide sequence and deduced amino acid sequence of the *Ca*GSTF. Stop codon is denoted by an asterisk. The intron sequence is in lower case. The underlined sequences are the primer sequences.

Gly88, Lys89, Thr90 and Thr119, all the other residues of *Ca*GSTF were scored positive (Fig. 4B) indicating they are reliably folded. The *Ca*GSTF showed a typical glutathione transferases structure, and constituted by two distinct domains; a smaller thioredoxin-like N-terminal domain (residues 1–79) and a larger helical C-terminal domain (residues 91–218). N-terminal domain and C-terminal domain were connected by a 11-residue linker (residues 80–90). The N-terminal domain constitutes roughly one-third of the protein and consists of a βαβαββα structural motif in which β3 is antiparallel with respect to the other β-strands (Fig. 4A). The C-terminal domain is composed entirely of six helices (α4 to α9). The α4 helix is disrupted by three amino acids (Gln106, Ser107 and Phe108). To keep the naming of the secondary structure consistent with other GST structures the two segments of α4 were named α4′ and α4″. The core of the C-terminal domain is a bundle of four helices (α4α5α6α7).

Despite of low protein sequence identity among plant GSTs, certain structural conservation is evident. The GSH-binding N-terminal domain is highly conserved. All the highly conserved residues in this domain should have specific functions. The X-ray structures of *Zea mays* phi GSTs *Zm*GSTI and *Zm*GSTIII (PDB: 1AXD and 1AW9) showed the Ser12 residue (alignment position 14 in Fig. 2) is the catalytic residue responsible for stabilisation of the thiolate anion of enzyme-bound glutathione. The *Ca*GSTF contains two serine residues, Ser12 and Ser13, in N-terminal domain. Sequence and structure comparison suggested Ser12 of *Ca*GSTF is GSH-binding (G-site) residue (Figs. 2 and 5). The X-ray structure of ZmGSTI indicates Lys42, Val55, Glu67 and Ser68 are G-site residues, which form the H-bonds with the GSH (Fig. 5). Lys42, Glu67 and Ser68 of *Zm*GSTI are highly conserved in plant phi GSTs (alignment positions 44, 69 and 70 in Fig. 2), except that Val55 of *Zm*GSTI is replaced by Ile in *Ca*GSTF and *Zm*GSTIII (alignment position 57 in Fig. 2). The four aforementioned residues in *Ca*GSTF correspond to the G-site residues in *Zm*GSTI (Fig. 5). Thus, Ser12, Lys42, Ile55, Glu67 and Ser68 of *Ca*GSTF were predicted as G-site residues. The catalytic properties of these residues were further investigated by site-directed mutagenesis in this study.

3.3. Expression and purification of the recombinant CaGSTF and mutants

The Ser12, Lys42, Ile55, Glu67 and Ser68 residues of *Ca*GSTF were individually replaced with alanine. DNA sequencing confirmed that all of the desired mutants were successfully generated. The *Ca*GSTF cDNA and all the mutant cDNA were subcloned into the pET30a plasmid to generate expression constructs. Induction of the *E. coli* BL21-Tuner transformed expression constructs resulted in overexpression of the recombinant protein (Fig. 6). The *Ca*GSTF and all mutants were expressed mainly as soluble proteins in *E. coli* at 20 °C (Fig. 6). Soluble recombinant proteins were purified by Ni^{2+} affinity

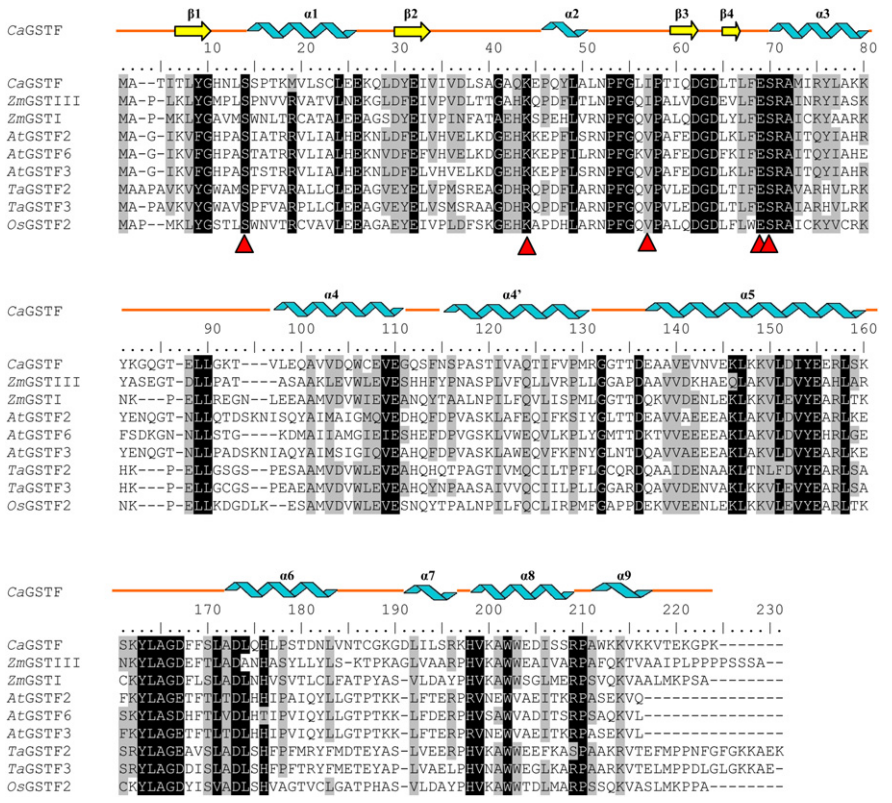

Fig. 2. Sequence alignment of plant phi GSTs and the predicted secondary structure elements of the *Ca*GSTF. Alpha helices and beta strands are represented as helices and arrows, respectively. Predicted G-site residues of *Ca*GSTF are marked with ▲ in red. Conserved residues in all plant phi GSTs are shaded. *Zm*GSTIII (*Zea mays*, GenBank accession number CAB38118); *Zm*GSTI (*Zea mays*, GenBank accession number NP_001105412); *At*GSTF2 (*Arabidopsis thaliana*, GenBank accession number 1GNW); *At*GSTF6 (*Arabidopsis thaliana*, GenBank accession number AAM19908); *At*GSTF3 (*Arabidopsis thaliana*, GenBank accession NP_178394); *Ta*GSTF2 (*Triticum aestivum*, GenBank accession number CAD29475); *Ta*GSTF3 (*Triticum aestivum*, GenBank accession number CAD29476); *Os*GSTF2 (*Oryza sativa*, GenBank accession number AAC64007). (For interpretation of the references to colour in this figure legend, the reader is referred to the web version of this article.)

column. Because the *Ca*GSTF gene and all mutants were inserted into the *Bam*HI and *Hind*III sites in the pET30a expression vector which provides the correct reading frame and a 6 × His-tag at the N-terminus, the theoretical molecular mass of the recombinant proteins should be 29.6 kDa. The molecular weights of the purified recombinant proteins were estimated to be approximately 30 kDa by SDS–PAGE analysis (Fig. 6).

3.4. Biochemical properties of the *Ca*GSTF and mutants

The specific activities measured for the *Ca*GSTF and all the mutants towards various substrates are listed in Table 1. The recombinant *Ca*GSTF and K42A mutant showed specific activities towards substrates 7-chloro-4-nitrobenzo-2-oxa-1,3-diazole (NBD-Cl) and 1-chloro-2,4-dinitrobenzene (CDNB). The *Ca*GSTF had much higher activities towards the two substrates than K42A mutant. However, the two proteins did not show any activity towards other GST substrates 4-nitrobenzyl chloride (NBC), hydroxyethyl disulphide (HED), dehydroascorbate (DHA) and cumene hydroperoxide (Cum-OOH). When the Ser12, Ile55, Glu67 and Ser68 residues of *Ca*GSTF were individually replaced with alanine, all mutants did not show any activity towards all substrates listed in Table 1.

The apparent kinetic constants of the recombinant *Ca*GSTF and K42A mutant were determined using NBD-Cl and GSH as substrates (Table 2). At fixed NBD-Cl concentration, the K_m^{GSH} values of *Ca*GSTF and K42A mutant were 0.35 mM and 1.56 mM, respectively, indicating *Ca*GSTF has much higher affinity (lower K_m^{GSH}) for GSH than K42A mutant. At fixed GSH concentration, the $K_m^{NBD\text{-}Cl}$ values of *Ca*GSTF and K42A mutant were 0.36 mM and 1.64 mM, respectively. The *Ca*GSTF showed 4.5 fold higher affinity (lower K_m^{GSH}) for xenobiotic substrate NBD-Cl than K42A mutant. The catalytic efficiencies (k_{cat}/K_m) of *Ca*GSTF were 11.2- and 17.7-fold higher than K42A mutant towards substrates GSH and NBD-Cl, respectively (Table 2).

The enzymatic activity of *Ca*GSTF is pH dependent. The optimum pH for *Ca*GSTF is around pH 6.5 using NBD-Cl as substrate (Fig. 7A). The enzyme had >20% of its maximum activity at pH range of 5.5–8.0. The enzyme's activity was nearly abolished at pH 5.0 and 9.5. Thus, *Ca*GSTF has optimal activity at acidic solution. In contrast, many plant phi GSTs show the optimum activity in basic solution, e.g. the optimum activity of rice *Os*GSTF3 and *Os*GSTF5 is at pH 9.0 (Cho and Kong, 2005; Cho et al., 2007); maize GST-IV at pH 7.8 (Irzyk and Fuerst, 1993). The K42A mutant showed similar optimum pH (Fig. 7A).

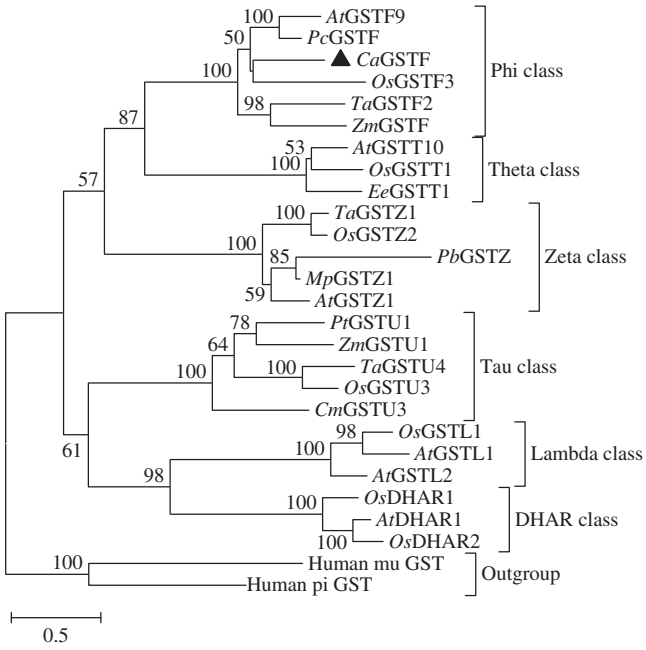

Fig. 3. Phylogenetic relationships between *Ca*GSTF and other classes of plant GSTs. The neighbour-joining method was used in the tree reconstruction. Bootstrap values from a sample of 1000 replicates are shown on each branch. The tree was rooted with *Homo sapiens* mu GST (GenBank accession number Q03013) and *Homo sapiens* pi GST (GenBank accession number P09211). The affiliations of the plant GST sequences used in the tree reconstruction are the following: *At*GSTF9 (*Arabidopsis thaliana*, GenBank accession number AAK49621); *Pc*GSTF (*Pyrus communis*, GenBank accession number ABI79308); *Os*GSTF3 (*Oryza sativa*, GenBank accession number AF309384); *Ta*GSTF2 (*Triticum aestivum*, GenBank accession number CAD29475); *Zm*GSTF (*Zea mays*, GenBank accession number NP_001105412); *At*GSTT10 (*Arabidopsis thaliana*, GenBank accession number CAA10457); *Os*GSTT1 (*Oryza sativa*, GenBank accession number AAK98534); *Ee*GSTT1 (*Euphorbia esula*, GenBank accession number AAF64449); *Ta*GSTZ1 (*Triticum aestivum*, GenBank accession number O04437); *Os*GSTZ2 (*Oryza sativa*, GenBank accession number AAK98533); *At*GSTZ1 (*Arabidopsis thaliana*, GenBank accession number NP_178344); *Mp*GSTZ1 (*Malva pusilla*, GenBank accession number AAO61856); *Pb*GSTZ (*Pinus brutia*, GenBank accession number GU270573); *Pt*GSTU1 (*Pinus tabulaeformis*, GenBank accession number AY640175); *Zm*GSTU1 (*Zea mays*, GenBank accession number CAA73369); *Ta*GSTU4 (*Triticum aestivum*, GenBank accession number 1GWCA); *Os*GSTU3 (*Oryza sativa*, GenBank accession number AAQ02687); *Gm*GSTU3 (*Glycine max*, GenBank accession number X68819); *Os*GSTL1 (*Oryza sativa*, GenBank accession number ABC74869); *At*GSTL1 (*Arabidopsis thaliana*, GenBank accession number NM_120356); *At*GSTL2 (*Arabidopsis thaliana*, GenBank accession NM_115362); *Os*DHAR1 (*Oryza sativa*, GenBank accession number AAL71856); *At*DHAR1 (*Arabidopsis thaliana*, GenBank accession number AY039590); *Os*DHAR2 (*Oryza sativa*, GenBank accession number BAD38160).

3.5. Structural changes

The thermal stability of the recombinant *Ca*GSTF and the K42A mutant was illustrated in Fig. 7B. *Ca*GSTF retained 56% of its initial activity at 35 °C, indicating *Ca*GSTF was stable below 35 °C. At 40 °C, the enzyme's activity was nearly abolished. The K42A mutant retained 67% of its initial activity at 40 °C, but it almost did not show any activity at 45 °C.

The anionic dye ANS is widely used for probing structural changes in proteins (Schonbrunn et al., 2000). When ANS was bound to the enzyme proteins, the fluorescence intensity was enhanced, accompanied by a blue shift in its fluorescence-emission maximum from 520 nm (free ANS in buffer) to 500 nm for the *Ca*GSTF and all mutant proteins (Fig. 8). Compared with the wild-type protein, there was no change in the emission maximum wavelength of ANS bound to all mutants (Fig. 8). The ANS fluorescence intensities of the S12A, K42A, E67A and S68A mutants were higher than the wild-type protein. But, The I55A mutant and wild-type *Ca*GSTF showed almost identical fluorescence spectra, indicating that I55A mutant shared similar structure with wild-type enzyme.

4. Discussion

In this study, we cloned and characterized a phi GST (*Ca*GSTF) from *C. argyrophylla*. Based on the N-terminal amino acid sequence identity to the available crystal structures of plant phi GSTs, Ser12, Lys42, Ile55, Glu67 and Ser68 of *Ca*GSTF were proposed as G-site residues. The conserved Ser12 residue of *Ca*GSTF (alignment position 14 in Fig. 2) is observed in plant tau, zeta and theta class GSTs (Zeng et al., 2005). This highly conserved amino acid is thought to be the catalytic residue responsible for stabilisation of the thiolate anion of enzyme-bound GSH (Armstrong, 1997; Thom et al., 2001). Mutation of this Ser residue in pine *Pt*GSTU1 and rice *Os*GSTU17 led to abolishment of the enzymatic activity (Yang et al., 2009; Zeng et al., 2005). In this study, after replacing Ser12 of *Ca*GSTF by alanine, the mutant S12A also did not show any activity, indicating this Ser residue is critical for catalysis. In a natural occurring tomato tau GST *Le*GSTU1 where the Ser13 is replaced by Gly (Kilili

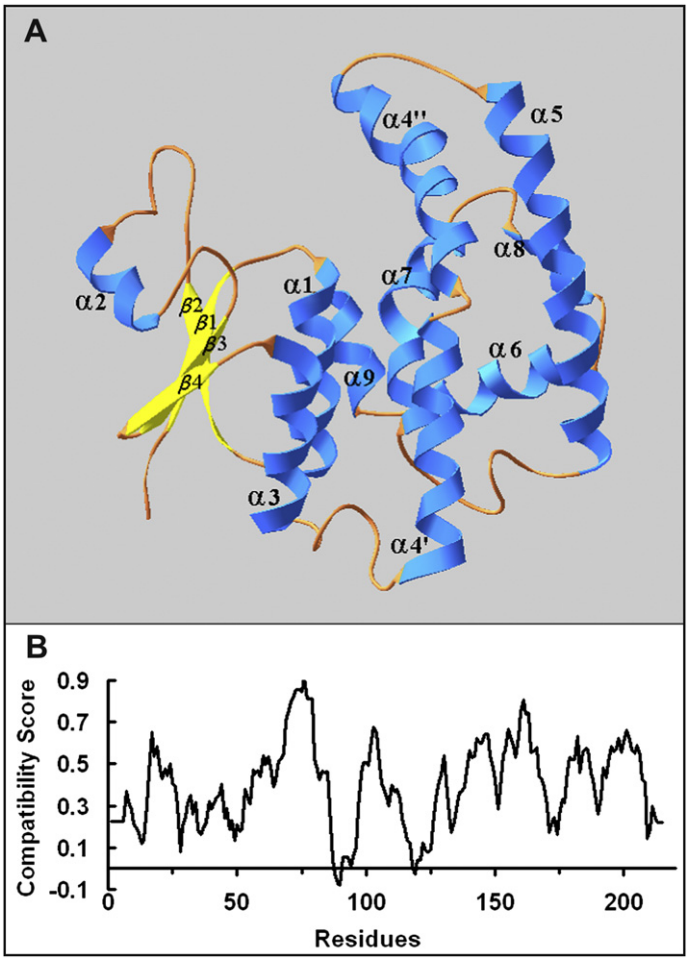

Fig. 4. Predicted three-dimensional structure of *Ca*GSTF (A) and the evaluation of the structure by Profile-3D program (B). Alpha helices and beta strands are represented as blue helices and yellow arrows, respectively. The three-dimensional structural image was generated using the program Swiss-Pdb Viewer. (For interpretation of the references to colour in this figure legend, the reader is referred to the web version of this article.)

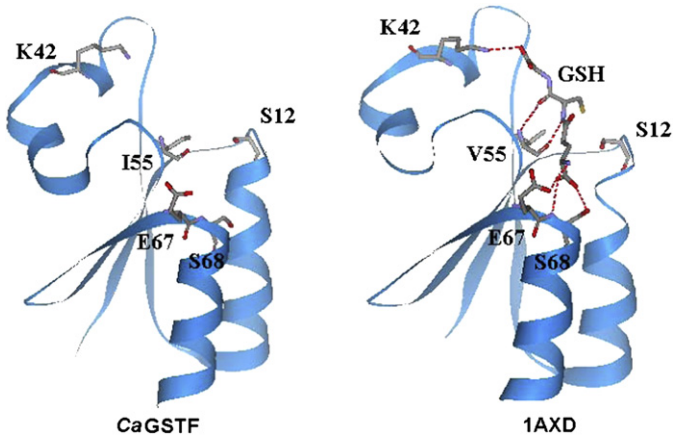

Fig. 5. Structural comparison of the N-terminal domain between *Ca*GSTF and maize phi GSTI. Protein data bank code and reference for the maize phi GSTI structure are 1AXD (Neuefeind et al., 1997). The red broken line represents the hydrogen bond. These images were generated using the program Discovery Studio. (For interpretation of the references to colour in this figure legend, the reader is referred to the web version of this article.)

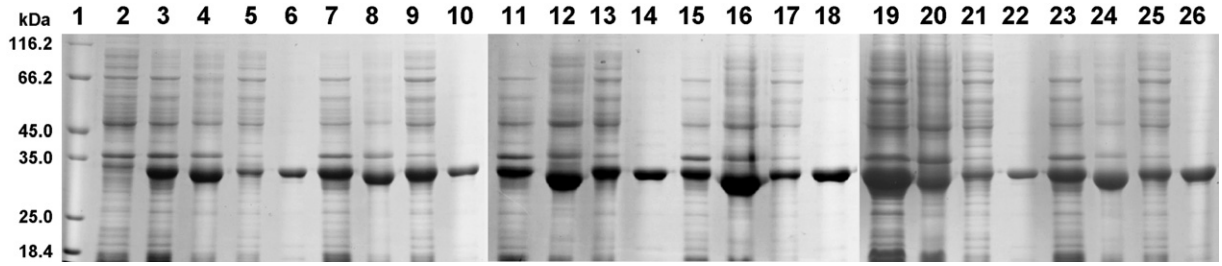

Fig. 6. SDS–PAGE analysis of the recombinant *Ca*GSTF and mutants. Lane 1, molecular mass markers with the sizes shown on the left in kilodaltons; lane 2, total cellular extract from *E. coli*; lanes 3, 7, 11, 15, 19 and 23, total cellular extracts from induced bacteria containing *Ca*GSTF, and the mutants S12A, K42A, I55A, E67A and S68A, respectively; lanes 4, 8, 12, 16, 20 and 24, supernatant after ultrasonication and centrifugation of cells expressing recombinant *Ca*GSTF and the mutants S12A, K42A, I55A, E67A and S68A proteins, respectively; lanes 5, 9, 13, 17, 21 and 25, cell pellet after ultrasonication and centrifugation of cells expressing recombinant *Ca*GSTF and the mutants S12A, K42A, I55A, E67A and S68A proteins, respectively; lanes 6, 10, 14, 18, 22 and 26, the purified recombinant *Ca*GSTF and the mutants S12A, K42A, I55A, E67A and S68A proteins, respectively.

Table 1
Specific activities of the wild type and mutants of *Ca*GSTF towards different substrates. The values shown are means ± S.D., calculated from three replicates.

GSTs	Specific activity (μmol/min per mg)					
	NBD-Cl	CDNB	NBC	DHA	HED	Cum-OOH
*Ca*GSTF	1.92 ± 0.03	0.18 ± 0.01	n.d.	n.d.	n.d.	n.d.
S12A	n.d.	n.d.	n.d.	n.d.	n.d.	n.d.
K42A	0.48 ± 0.01	0.09 ± 0.01	n.d.	n.d.	n.d.	n.d.
I55A	n.d.	n.d.	n.d.	n.d.	n.d.	n.d.
E67A	n.d.	n.d.	n.d.	n.d.	n.d.	n.d.
S68A	n.d.	n.d.	n.d.	n.d.	n.d.	n.d.

et al., 2004), the enzyme showed very poor activity in GSH conjugation reactions with CDNB (0.07 μmol min^{-1} protein mg^{-1}) (Kilili et al., 2004), which further confirms the essential role of this residue in GST catalysis.

Glu66 and Ser67 (alignment positions 69 and 70 in Fig. 2) of *Ca*GSTF are conserved in the plant phi GSTs (Fig. 2). The two conserved residues were observed in plant tau, zeta and theta class GSTs (Zeng and Wang, 2005). The X-ray structures of *Z. mays* phi GSTs *Zm*GSTI (PDB: 1AXD) showed the two residues interact with GSH through hydrogen bonds (Fig. 5). Removing the side chains of the two residues in pine *Pt*GSTU1 significantly affects the enzyme's substrate specificity and affinity for GSH. In this study, the mutants E67A and S68A did not show any activity towards test substrates, indicating the two conserved residues were essential for catalytic function of *Ca*GSTF. The ANS fluorescence intensities of the E67A and S68A mutants were higher than the wild-type protein, indicating that removing the side chains of the two residues may affect the conformation of the GSH-binding pocket. In contrast, the I55A mutant showed almost identical fluorescence spectra with *Ca*GSTF protein, indicating that removing the side chain of Ile55 did not affect the structure of wild-type enzyme. However, the I55A mutant did not show any activity towards test substrates, indicating this residue play an important role in catalytic function of *Ca*GSTF.

Lys42 of *Ca*GSTF is located in the loop connecting the β-strand 2 to α-helix 2 in the N-terminal domain (Fig. 2). After replacing Lys42 of *Ca*GSTF by alanine, the mutant K42A showed the higher ANS fluorescence intensity than the wild-type protein. The crystal structures of *Z. mays* phi GSTs *Zm*GSTI show that the side chain of the amide nitrogen of this Lys residue forms a hydrogen bond with the carboxylate oxygen atom of the Gly residue of GSH (Fig. 5). Removing the side chain of Lys42 in *Ca*GSTF would prevent formation of the hydrogen bond between Lys42 and GSH, which in turn would affect the interactions of the enzyme with GSH. Thus, compared to wild-type enzyme, the mutant K42A showed very low affinity towards GSH and very low activities towards substrates CDNB and NBD-Cl.

*Ca*GSTF showed low specific activities towards substrate CDNB and NBD-Cl. This is in contrast to other phi GSTs from wheat (Cummins et al., 2003), sorghum (Gronwald and Plaisance, 1998), maize and soybean (McGonigle et al., 2000), in which high specific activity towards substrate CDNB and other xenobiotics are reported. Comparison to other conifer phi GSTs cannot be made since there is no other study yet available. Our previous investigations targeted on four tau GSTs cloned from *Pinus tabulaeformis*, *Pinus yunnanensis* and *Pinus densata*, and revealed high specific activities towards CDNB, NBD-Cl and ECA for all

Table 2
Kinetic constants of the recombinant *Ca*GSTF and K42A mutants using NBD-Cl and GSH as substrates. The values shown are means ± S.D., calculated from three replicates.

GSTs	GSH			NBD-Cl		
	K_m (mM)	k_{cat} (S^{-1})	k_{cat}/K_m (mM^{-1} S^{-1})	K_m (mM)	k_{cat} (S^{-1})	k_{cat}/K_m (mM^{-1} S^{-1})
*Ca*GSTF	0.35 ± 0.01	3.40	9.82	0.36 ± 0.03	5.41	15.14
K42A	1.56 ± 0.11	1.36	0.87	1.64 ± 0.37	1.39	0.85

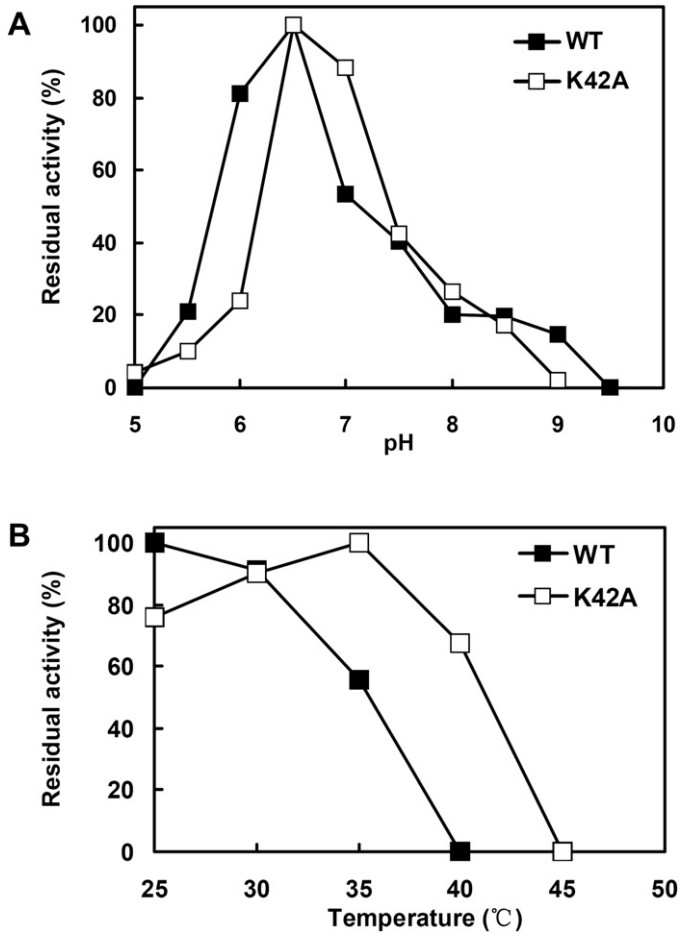

Fig. 7. Biochemical characterization of the recombinant *Ca*GSTF and the K42A mutant. Effect of pH on NBD-Cl-conjugating activities of *Ca*GSTF and the K42A mutant (A); and thermal stability of *Ca*GSTF and the K42A mutant (B) based on the retention of enzymatic activity towards the substrate NBD-Cl following heat treatments.

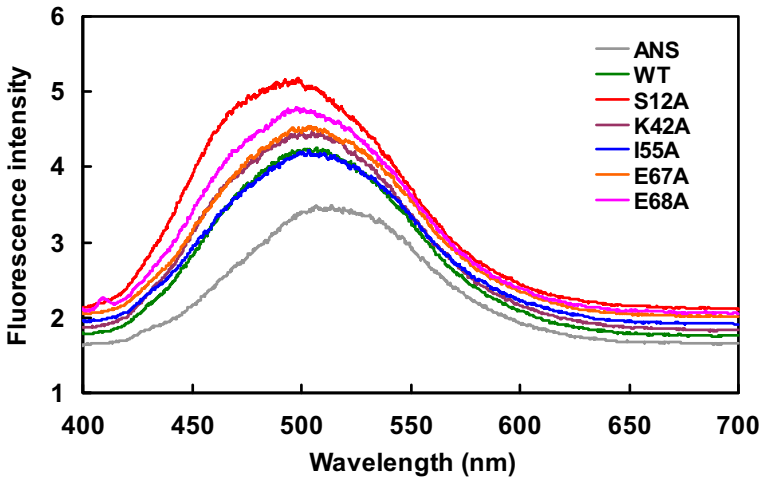

Fig. 8. Fluorescence-emission spectra of ANS binding to the K42A mutant and wild-type *Ca*GSTF.

of them (Zeng et al., 2005; Zeng and Wang, 2006). Similarly, unclassified GSTs purified directly from needles of *Pinus mugo*, *Picea abies* and *P. glauca* also showed high specific activity towards CDNB and other substrates (Schroder and Berkau, 1993; Schroder et al., 1990; Schroder and Rennenberg, 1992). Thus, compared to conifer tau GSTs and other plant phi GSTs, *Ca*GSTF displayed a narrow substrate spectrum.

From other reports on plant phi GSTs, the apparent K_m^{GSH} values for GSH vary from 0.12 to 0.64 mM (Cho et al., 2007; Cummins et al., 2003; Gronwald and Plaisance, 1998; Irzyk and Fuerst, 1993; Lo Piero et al., 2006). The K_m^{GSH} value of *Ca*GSTF is 0.35 mM, suggesting that *Ca*GSTF had similar affinity for GSH with other plant phi GSTs. However, the *Ca*GSTF had low catalytic efficiency ($k_{cat}/K_m = 9.82$) for the substrates GSH (Table 2), which is far lower than that of the pine *Pt*GSTU1 (484.80), *Pt*GSTU2 (144.75) and wheat phi GSTs *Ta*GSTF1 (377.22), *Ta*GSTF3 (110.62) and *Ta*GSTF6 (88.06) (Cummins et al., 2003; Zeng et al., 2005). In this study, *Ca*GSTF showed thermolabile characteristic, without any enzyme's activity at 40 °C. In contrast, the other reported tau GSTs from conifers retained more than 60% of their initial activity at 45 °C (Zeng and Wang, 2005, 2006). High thermal stability is also observed in two rice phi GSTs (Cho and Kong, 2005; Cho et al., 2007).

The above biochemical analyses revealed unique characteristics of *Ca*GSTF from *C. argyrophylla*: it is thermolabile, has a narrow substrate spectrum, low catalytic efficiency and a different pH optimum profile than other angiosperm phi GSTs and conifer tau GSTs so far reported. These conspicuous properties of *Ca*GSTF imply ineffectiveness of the enzyme in detoxification metabolism and, thus, might entail insignificant functional role in the organism's adaptation to environmental stresses in the subtropical regions. Although it is attempting to draw this functional association, more investigations into other potential biochemical properties of *Ca*GSTF and on all the members of the gene family are necessary before any functional implications can be properly established. Nonetheless, the discovery of atypical properties of the first phi GST from *C. argyrophylla* is in its own right interesting enough for further gene family evolution examinations.

Acknowledgements

This study was supported by grants from National Basic Research Program of China (2009CB119104), the Knowledge Innovation Program of the Chinese Academy of Sciences (KSCX2-EW-J-1) and Natural Science Foundation of China (NSFC 30830010).

References

Armstrong, R.N., 1997. Structure, catalytic mechanism, and evolution of the glutathione transferases. Chem. Res. Toxicol. 10, 2–18.
Basantani, M., Srivastava, A., 2007. Plant glutathione transferases – a decade falls short. Can. J. Bot. 85, 443–456.
Cho, H.Y., Kong, K.H., 2005. Molecular cloning, expression, and characterization of a phi-type glutathione S-transferase from *Oryza sativa*. Pestic. Biochem. Physiol. 83, 29–36.
Cho, H.Y., Lee, H.J., Kong, K.H., 2007. A phi class glutathione S-transferase from *Oryza sativa* (OsGSTF5): molecular cloning, expression and biochemical characteristics. J. Biochem. Mol. Biol. 40, 511–516.
Cummins, I., O'Hagan, D., Jablonkai, I., Cole, D.J., Hehn, A., Werck-Reichhart, D., Edwards, R., 2003. Cloning, characterization and regulation of a family of phi class glutathione transferases from wheat. Plant Mol. Biol. 52, 591–603.
Dirr, H., Reinemer, P., Huber, R., 1994. X-ray crystal structures of cytosolic glutathione S-transferases. Implications for protein architecture, substrate recognition and catalytic function. Eur. J. Biochem. 220, 645–661.
Dixon, D., Cole, D.J., Edwards, R., 1997. Characterisation of multiple glutathione transferases containing the GST I subunit with activities toward herbicide substrates in maize (*Zea mays*). Pestic. Sci. 50, 72–82.
Dixon, D.P., Lapthorn, A., Edwards, R., 2002. Plant glutathione transferases. Genome Biol. 3 reviews 3004.3001–3004.3010.
Edwards, R., Dixon, D.P., 2005. Plant glutathione transferases. Methods Enzymol. 401, 169–186.
Edwards, R., Dixon, D.P., Walbot, V., 2000. Plant glutathione S-transferases: enzymes with multiple functions in sickness and in health. Trends Plant Sci. 5, 193–198.
Frova, C., 2003. The plant glutathione transferase gene family: genomic structure, functions, expression and evolution. Physiol. Plant. 119, 469–479.
Gronwald, J.W., Plaisance, K.L., 1998. Isolation and characterization of glutathione S-transferase isozymes from sorghum. Plant Physiol. 117, 877–892.
Habig, W.H., Pabst, M.J., Jakoby, W.B., 1974. Glutathione S-transferases. The first enzymatic step in mercapturic acid formation. J. Biol. Chem. 249, 7130–7139.
Hall, T.A., 1999. BioEdit: a user-friendly biological sequence alignment editor and analysis program for Windows 95/98/NT. Nucl. Acids Symp. Ser. 41, 95–98.
Irzyk, G.P., Fuerst, E.P., 1993. Purification and characterization of a glutathione S-transferase from benoxacor-treated maize (*Zea mays*). Plant Physiol. 102, 803–810.
Kilili, K.G., Atanassova, N., Vardanyan, A., Clatot, N., Al-Sabarna, K., Kanellopoulos, P.N., Makris, A.M., Kampranis, S.C., 2004. Differential roles of tau class glutathione s-transferases in oxidative stress. J. Biol. Chem. 279, 24540–24551.
Layne, E., 1957. Spectrophotometric and turbidimetric methods for measuring proteins. Methods Enzymol. 3, 447–455.
Lo Piero, A.R., Puglisi, I., Petrone, G., 2006. Gene isolation, analysis of expression, and in vitro synthesis of glutathione S-transferase from orange fruit *Citrus sinensis* L. (Osbeck). J. Agric. Food Chem. 54, 9227–9233.
McGonigle, B., Keeler, S.J., Lau, S.M., Koeppe, M.K., O'Keefe, D.P., 2000. A genomics approach to the comprehensive analysis of the glutathione S-transferase gene family in soybean and maize. Plant Physiol. 124, 1105–1120.
Neuefeind, T., Huber, R., Dasenbrock, H., Prade, L., Bieseler, B., 1997. Crystal structure of herbicide-detoxifying maize glutathione S-transferase-I in complex with lactoylglutathione: evidence for an induced-fit mechanism. J. Mol. Biol. 274, 446–453.
Oakley, A.J., 2005. Glutathione transferases: new functions. Curr. Opin. Struct. Biol. 15, 716–723.
Oztetik, E., 2005. Purification of Glutathione S-transferases and Genetic Characterization of Zeta Isozyme from *Pinus brutia*, Ten. Department of Biochemistry, Middle East Technical University, Ankara, Turkey.
Öztetik, E., 2008. A tale of plant glutathione *S*-transferases: since 1970. Bot. Rev. 74, 419–437.
Ricci, G., Caccuri, A.M., Lo Bello, M., Pastore, A., Piemonte, F., Federici, G., 1994. Colorimetric and fluorometric assays of glutathione transferase based on 7-chloro-4-nitrobenzo-2-oxa-1,3-diazole. Anal. Biochem. 218, 463–465.
Sappl, P.G., Onate-Sanchez, L., Singh, K.B., Millar, A.H., 2004. Proteomic analysis of glutathione S-transferases of *Arabidopsis thaliana* reveals differential salicylic acid-induced expression of the plant-specific phi and tau classes. Plant Mol. Biol. 54, 205–219.
Schonbrunn, E., Eschenburg, S., Luger, K., Kabsch, W., Amrhein, N., 2000. Structural basis for the interaction of the fluorescence probe 8-anilino-1-naphthalene sulfonate (ANS) with the antibiotic target MurA. Proc. Natl. Acad. Sci. U. S. A. 97, 6345–6349.
Schroder, P., Berkau, C., 1993. Characterization of cytosolic glutathione S-transferase in spruce needles. Bot. Acta 106, 301–306.

Schroder, P., Lamoureux, G.L., Rusness, D.G., Rennenberg, H., 1990. Glutathione S-transferase activity in spruce needles. Pestic. Biochem. Physiol. 37, 211–218.
Schroder, P., Rennenberg, H., 1992. Characterization of glutathione S-transferase from dwarf pine needles (*Pinus mugo* Turra). Tree Physiol. 11, 151–160.
Soranzo, N., Sari Gorla, M., Mizzi, L., De Toma, G., Frova, C., 2004. Organisation and structural evolution of the rice glutathione S-transferase gene family. Mol. Genet. Genom. 271, 511–521.
Tamura, K., Dudley, J., Nei, M., Kumar, S., 2007. MEGA4: molecular evolutionary genetics analysis (MEGA) software version 4.0. Mol. Biol. Evol. 24, 1596–1599.
Thom, R., Dixon, D.P., Edwards, R., Cole, D.J., Lapthorn, A.J., 2001. The structure of a zeta class glutathione S-transferase from *Arabidopsis thaliana*: characterisation of a GST with novel active-site architecture and a putative role in tyrosine catabolism. J. Mol. Biol. 308, 949–962.
Thompson, J.D., Gibson, T.J., Plewniak, F., Jeanmougin, F., Higgins, D.G., 1997. The Clustal X windows interface: flexible strategies for multiple sequence alignment aided by quality analysis tools. Nucl. Acids Res. 24, 4876–4882.
Wang, H.W., Ge, S., 2006. Phylogeography of the endangered *Cathaya argyrophylla* (Pinaceae) inferred from sequence variation of mitochondrial and nuclear DNA. Mol. Ecol. 15, 4109–4122.
Wu, J.R., Cramer, C.L., Hatzios, K.K., 1999. Characterization of two cDNAs encoding glutathione S-transferases in rice and induction of their transcripts by the herbicide safener fenclorim. Physiol. Plant. 105, 102–108.
Wu, Z.Y., Peter, H.R., 1999. Flora of China. Science Press, Beijing.
Yang, X., Sun, W., Liu, J.P., Liu, Y.J., Zeng, Q.Y., 2009. Biochemical and physiological characterization of a tau class glutathione transferase from rice (*Oryza sativa*). Plant Physiol. Biochem. 47, 1061–1068.
Yuen, W.K., Ho, J.W., 2001. Purification and characterization of multiple glutathione S-transferase isozymes from *Chironomidae larvae*. Comp. Biochem. Physiol. A Mol. Integr. Physiol. 129, 631–640.
Zeng, Q.Y., Lu, H., Wang, X.R., 2005. Molecular characterization of a glutathione transferase from *Pinus tabulaeformis* (Pinaceae). Biochimie 87, 445–455.
Zeng, Q.Y., Wang, X.R., 2005. Catalytic properties of glutathione-binding residues in a tau class glutathione transferase (PtGSTU1) from *Pinus tabulaeformis*. FEBS Lett. 579, 2657–2662.
Zeng, Q.Y., Wang, X.R., 2006. Divergence in structure and function of tau class glutathione transferase from *Pinus tabulaeformis*, *P. yunnanensis* and *P. densata*. Biochem. Syst. Ecol. 34, 678–690.